Frontiers in Bioscience Landmark

Front. Biosci. (Landmark Ed) **2025**; 30(4): 26038
https://doi.org/10.31083/FBL26038

Original Research

Sesamin Exerts Anti-Tumor Activity in Nasopharyngeal Carcinoma Through Inducing Autophagy and Reactive Oxygen Species Production

Deqiang An[1], Xianyao Jiang[1], Yucheng Yang[1,*]

[1]Department of Otorhinolaryngology, The First Affiliated Hospital of Chongqing Medical University, 400016 Chongqing, China
*Correspondence: YuchengYangabc@163.com (Yucheng Yang)
Academic Editor: Amedeo Amedei
Submitted: 7 August 2024 Revised: 15 November 2024 Accepted: 26 November 2024 Published: 25 April 2025

Abstract

Background: Sesamin can suppress many cancers, but its effect on nasopharyngeal carcinoma (NPC) is unclear. Herein, we set out to pinpoint the possible changes in NPC due to Sesamin. **Methods**: The biological function of NPC cells exposed to Sesamin/N-acetyl-L-cysteine (NAC)/3-Methyladenine (3-MA) was detected, followed by evaluation of reactive oxygen species (ROS) production (dichlorodihydrofluorescein diacetate staining) and mitochondrial membrane potential (MMP) (flow cytometry). Proteins pertinent to apoptosis (cleaved caspase-3, cleaved poly (ADP-ribose) polymerase 1 (PARP1)), cell cycle (Cyclin B1), and autophagy (microtubule-associated protein light chain 3 (LC3)-I, LC3-II, Beclin-1, P62) were quantified by Western blot. After the xenografted tumor model in mice was established, the tumor volume and weight were recorded, and Ki-67 and cleaved caspase-3 levels were determined by immunohistochemical analysis. **Results**: Sesamin inhibited viability, proliferation, cell cycle progression and migration, induced apoptosis, increased ROS production, and decreased MMP in NPC cells. Sesamin elevated cleaved caspase-3/caspase-3, cleaved PARP1/PARP1, and Beclin-1 expressions as well as LC3-II/LC3-I ratio, while diminishing Cyclin B1 and P62 levels. NAC and 3-MA abrogated Sesamin-induced changes as above in NPC cells. Sesamin inhibited the increase of the xenografted tumor volume and weight, down-regulated Ki-67, and up-regulated cleaved caspase-3 in xenografted tumors. **Conclusion**: Sesamin exerts anti-tumor activity in NPC, as demonstrated by attenuated tumor proliferation and xenografted tumor volume and weight, as well as induced apoptosis in tumor tissues, consequent upon the promotion of autophagy and reactive oxygen species production.

Keywords: nasopharyngeal carcinoma; sesamin; autophagy; reactive oxygen species; xenografted tumors

1. Introduction

Nasopharyngeal carcinoma (NPC), a malignancy occurring on the epithelium of the nasopharyngeal mucosal lining, is the most prevalent type of cancer in the head and neck regions [1,2]. Although NPC is relatively uncommon compared with other cancers, with only new cases (129,000) representing 0.7% of all cancer diagnoses, advanced NPC is pertinent to 38%–63% of the overall 5-year survival rate [3,4]. Conventionally, treatment modalities for NPC encompass radiotherapy, chemotherapy, surgery and targeted therapy, and immunotherapy has gained traction as an additional strategy for advanced NPC in recent years [5]. Despite advancements in clinical treatment methods, 19–29% of patients still experience post-radiotherapy relapse and distant metastasis, which adversely affects survival and life quality, primarily due to radiotherapy resistance [6]. Therefore, the pursuit of innovative and effective pharmaceuticals for NPC treatment is of paramount importance.

Of note, increasing evidence has underscored the significance of natural products in combating various cancer types including NPC because these products are valued for multi-channel, multi-point, multi-effect, minimal side effect properties, and so on [7–9]. For instance, Dihydroartemisinin, Luteolin, and Cruciferae sulforaphane are anti-NPC candidate drugs [9–11]. Sesamin, a major active ingredient in Sesame, also exists in some other plants, such as Araliaceae, Rutaceae, and Scrophulariaceae [12]. Given the widespread culinary uses of Sesame, many researchers in East Asia have widely studied its active constituents including Sesamin [13], thus revealing plentiful biological activities of Sesamin such as anti-oxidation, anti-inflammation, and anti-lipogenesis [14–16]. Furthermore, Sesamin has been greatly reported to possess powerful anti-tumor effects [17]. For example, it has been confirmed to repress proliferation and enhance apoptosis of non-small cell lung cancer cells by modulating protein kinase B (AKT)/p53 signaling pathway [18], to suppress breast cancer development via inhibiting programmed death-ligand 1 (PD-L1) expression [19], and to induce the endoplasmic reticulum stress-mediated apoptosis and activating autophagy in cervical cancer cells [15]. However, whether Sesamin has the same anti-cancer effect on NPC has not been investigated as far as we know. Interestingly, studies showed that activating phosphoinositide 3-kinase (PI3K)-AKT or p53 signaling pathways can enhance the carcinogenicity or radiosensitivity of NPC [20,21]. PD-1/PD-L1 pathway is a possible immune-evasion mechanism pertinent to Epstein–Barr virus (EBV)-associated NPC [22]. Moreover, autophagy and apoptosis can be promoted in

NPC by inducing endoplasmic reticulum stress [23]. Accordingly, we conjectured that Sesamin may also exhibit growth-inhibiting properties in NPC.

Therefore, in the present study, we cultured NPC cell lines and established a xenografted-NPC-tumor mice model. After treatment of the cells and mice with Sesamin, the effects of Sesamin on cell tumorigenicity and tumor growth were further determined through a series of biological testing methods. Through the current research, we attempted to contribute new theoretical insights into Sesamin's properties and to provide novel treatment approaches for NPC.

2. Methods

2.1 Cell Culture

Human immortalized nasopharyngeal epithelial cell line NP69 (BFN60870097, BLUEFBIO, Shanghai, China) and human NPC cell lines including C666-1 (BFN608006727, BLUEFBIO, Shanghai, China) and HK-1 (JNO-H0105, Jennio, Guangzhou, China) were cultured (37 ℃, 5% CO_2) in Dulbecco's modified eagle medium (DMEM) (A4192101, Gibco, Waltham, MA, USA) supplemented with 10% fetal bovine serum (FBS) (16140071, Gibco). The cells used in this study were identified via short tandem repeat (STR) and the test results for mycoplasma were negative.

2.2 Drug Treatment

For the treatment of Sesamin alone, NP69, C666-1, and HK-1 cells were directly cultured (24 h) in Sesamin (10, 20, 50, 100, 200 µmol/L) ($C_{20}H_{18}O_6$, Purity: 99.70%, HY-N0121, MedChemExpress, Shanghai, China) and then collected for other experiments.

Then, HK-1 cells were assigned into 6 groups: Control (24-hour culture in DMEM with 10% FBS); N-acetyl-L-cysteine (NAC) (2-hour culture in 5 mM of NAC (S0077, Beyotime, Shanghai, China) and then 24-hour culture in DMEM with 10% FBS); 3-Methyladenine (3-MA) (2-hour culture in 3 mM 3-MA (M9281, Sigma, St. Louis, MO, USA) and then 24-hour culture in DMEM with 10% FBS); Sesamin (24-hour culture in 50 µmol/L Sesamin); Sesamin+NAC (2-hour culture in 5 mM of NAC and 24-hour culture in 50 µmol/L Sesamin); and Sesamin+3-MA (2-hour culture in 3 mM of 3-MA and 24-hour culture in 50 µmol/L Sesamin).

2.3 Cell Viability Detection

Methylthiazolyldiphenyl-tetrazolium bromide (MTT) assay kit (M1020, Solarbio, Beijing, China) was used in the cell viability detection. After 24-hour treatment with Sesamin (different concentrations), NP69, C666-1, and HK-1 cells were incubated in a 96-well with the 90 µL fresh FBS-free medium and 10 µL MTT solution (4 h), followed by a 10-minute reaction with 110 µL formazan dissolvent. Finally, the absorbance (490 nm) was obtained by employing an Imark microplate reader (Bio-Rad, Hercules, CA, USA). Relative cell viability (%) = (experimental group OD – blank group OD)/(control group OD – blank group OD) × 100%; values were then normalized against controls.

2.4 Cell Migration Detection

Transwell assay was conducted in this part. Sesamin-treated C666-1 and HK-1 cells (both 1.5×10^5) were suspended with 200 µL FBS-free DMEM. Transwell chambers (354234, Corning Life Sciences, Corning, NY, USA) were inserted into a 24-well plate. After the cells were placed into the chamber, 5% FBS-containing DMEM (700 µL) was added to the plate. After 24 h, the cells invading the lower chamber underwent fixation (4% paraformaldehyde fixative; P0099, Beyotime, Shanghai, China), and dyeing (crystal violet, 15 min; C110704, Aladdin, Shanghai, China). Finally, observation and data analysis were performed using the optical microscope (DM4M, Leica, Solms, Germany) and Image J 1.8.0 software (NIH, Bethesda, MD, USA), respectively. The comparison was performed using data normalization with the control group.

2.5 Reactive Oxygen Species (ROS) Detection

Dichlorodihydrofluorescein diacetate (DCFH-DA) staining was carried out for ROS detection. Sesamin/NAC/3-MA-treated C666-1 and HK-1 cells were subjected to washing with phosphate-buffered saline (PBS) thrice, followed by incubation with DCFH-DA staining buffer (S0033M, Beyotime, Shanghai, China) (30 min, 37 ℃). 2-(4-Amidinophenyl)-6-indolecarbamidine dihydrochloride (DAPI, Blue, C1002, Beyotime, Shanghai, China) was used to stain nuclei for 5 min. The observation was completed under a STELLARIS 5 laser confocal microscope (×200, Leica, Solms, Germany). The ROS level is represented by the fluorescence intensity of DCF. The comparison was performed using data normalization with the control group. The quantitation of mean fluorescence intensity through ImageJ (version 1.48v, NIH, Bethesda, MD, USA) was used to compare the ROS changes.

2.6 Mitochondrial Membrane Potential (MMP) Detection

Evaluation and analyses were accomplished via JC-1 staining and flow cytometry, respectively. Sesamin/NAC/3-MA-treated C666-1 and HK-1 cells were subjected to PBS washing (three times), followed by 20-minute incubation with JC-1 staining buffer (C2006, Beyotime, Shanghai, China) (37 ℃). Finally, cell MMP was dissected using a FACSCalibur™ flow cytometer (BD Biosciences, Franklin Lake, NJ, USA).

2.7 Cell Proliferation Detection

Colony formation assays were performed. Sesamin/NAC/3-MA-treated C666-1 and HK-1 cells were washed with PBS three times. Then, the cells (1.0×10^4) were resuspended in 2 mL 10% FBS-containing

DMEM. A total of 200 µL cell resuspension in each well of a 6-well plate underwent a 14-day culture, and cell colonies were first fixed (4% paraformaldehyde fixative) and then stained (crystal violet) for 15 min. Following the removal of extra crystal violet using PBS three times, cell colonies were photographed with a camera (D-LUX7, Leica, Weztlar, Germany), and quantified using Image J 1.8.0 software. The comparison was performed using data normalization with the control group.

2.8 Cell Cycle Detection

In this part, propidium iodide (PI) staining and flow cytometry were carried out. Sesamin/NAC/3-MA-treated C666-1 and HK-1 cells were washed with PBS three times, followed by 1-hour fixation (75% pre-cooling ethanol, M058838, MREDA, Beijing, China), 25-minute color development (PI buffer, ST511, Beyotime, Shanghai, China), and cell cycle distribution dissection (a flow cytometer).

2.9 Cell Apoptosis Detection

Using Annexin-V-FITC/propidium iodide (PI) staining and flow cytometry, cell apoptosis was examined. Following PBS washing thrice, Sesamin/NAC/3-MA-treated C666-1 and HK-1 cells were exposed to Annexin-V-FITC (C1062S, Beyotime, Shanghai, China) and PI (30 min, darkness). Finally, dissection on cell cycle distribution was completed by utilising a flow cytometer.

2.10 Western Blot

Post PBS washing thrice, Sesamin/NAC/3-MA-treated C666-1 and HK-1 cells were exposed to NP-40 (P0013F, Beyotime, Shanghai, China) (15 min) on ice and centrifuged (20 min, 14,000 $\times g$) for total protein collection. After protein concentration determination (bicinchoninic acid assay (BCA) kit, P0009, Beyotime, Shanghai, China), 25 µg of proteins that were separated on sodium dodecyl sulfate-polyacrylamide gel electrophoresis (SDS-PAGE) gels (P0052A, Beyotime, Shanghai, China) were transferred transferred to polyvinylidene difluoride membranes (ISEQ00010, Millipore, Billerica, MA, USA). After a 2-hour blockage (5% defatted milk, room temperature), membranes were incubated with primary (overnight, 4 ℃) and secondary (1.5 h, room temperature) antibodies (Abcam, Cambridge, UK): cleaved caspase-3 (1: 500, 17 kDa, ab2302), caspase-3 (1:5000, 32 kDa, ab32351), cleaved poly (ADP-ribose) polymerase 1 (PARP1) (1:5000, 25 kDa, ab32064), PARP1 (1:1000, 113 kDa, ab191217), Cyclin B1 (1:500, 55 kDa, ab72), microtubule-associated protein light chain 3 (LC-3)-I/II (1:3000, 16/18 kDa, ab51520), Beclin-1 (1:2000, 52 kDa, ab207612), P62 (1:10,000, 47 kDa, ab91526), and β-actin (1:5000, 42 kDa, ab8226), as well as rabbit (1:5000, ab205718) or mouse secondary antibody (1:5000, ab205719). The membrane was covered with developer solution (P0019, Beyotime, Shanghai, China) and the protein gray value was evaluated and anatomized using the Image Lab 3.0 Software (Bio-Rad, Hercules, CA, USA). The relative protein expression level = gray value of the target protein/gray value of β-actin. The comparison was performed using data normalization with the control group.

2.11 Establishment of Xenografted Tumor Mice Model

Eighteen female BALB/c nude mice (5–6 weeks old and 20 $\pm$ 2 g) were fed in the same specific pathogen-free environment with a 12-hour light/dark cycle, and diet obtained *ad libitum*. After a 5-day acclimation, three groups (n = 6/group) were set up based on the animals: the Model, the Sesamin-L, and the Sesamin-H.

Then, all mice received injection with 100 µL PBS containing 1×10^6 HK-1 cells via the right forelimb (above axillary fossa). After the cells were grown in the mice, gavage (once a day for 14 days) was separately performed on the Model, Sesamin-L, and Sesamin-H groups with 100 µL sterile normal saline (M051054, MREDA, Beijing, China), 50 mg/kg Sesamin, and 100 mg/kg Sesamin. Body weight and tumor volume measurements were performed every other day, and the tumor volume was calculated as follows: major diameter (L) $\times$ (minor diameter)^2 (W^2)/2 mm^3. On the last day, after anesthesia (5%, 50 mg/kg sodium pentobarbital; B005, Jiancheng Bioengineering, Nanjing, China) and euthanization (cervical dislocation), the tumors were collected, photographed, weighed, and further used for immunohistochemical analysis.

2.12 Immunohistochemical Analysis

After being photographed and weighed, the tumor tissue underwent fixation (24 h, paraformaldehyde fixative, P885233, MREDA, Beijing, China), transparentization (xylene, M056094, MREDA, Beijing, China), and paraffin embedding (M060593, MREDA, Beijing, China). A total of 4 µm tissue slices were prepared and dewaxed. Then, the slices were placed in an antigen repair buffer (M052013, MREDA, Beijing, China) and incubated with Ki-67 (1:500, ab15580, Abcam, Cambridge, UK) or cleaved caspase-3 (1:500, #9661, CST, Boston, MA, USA) antibodies (overnight, 4 ℃), and reacted (1 h) with rabbit antibody (ab205718, Abcam, Cambridge, UK). After DBA (SFQ004, 4A Biotech, Beijing, China) and hematoxylin (M1428, MREDA, Beijing, China) stainings, the slices were transparentized using xylene and sealed with neutral gum (M051989, MREDA, Beijing, China). Lastly, the tissue image ($\times$200) was recorded with an automatic DMLA microscope (Leica, Wetzlar, Germany). The comparison was performed using data normalization with the Model group.

2.13 Statistical Analysis

Multi-group comparisons were completed by employing one-way ANOVA. All statistical analyses were implemented using GraphPad Prism 8.0 software (GraphPad

Software, Inc., San Diego, CA, USA), with the final data described using Mean ± Standard Deviation. Tukey's multiple comparison test and Dunnett's multiple comparison test were used for statistical analyses. $p < 0.05$ was determined to be of statistical significance.

3. Results

3.1 Sesamin Reduced Viability and Proliferation While Inducing Apoptosis of NPC Cells

Fig. 1A exhibited the chemical structure of Sesamin. The means of how Sesamin influences the viability of normal NP69 cells (Fig. 1B), as well as NPC C666-1 cells (Fig. 1C) and HK-1 cells (Fig. 1D), were determined. The results showed that 10/20/50 µmol/L Sesamin did not affect NP69 cell viability (Fig. 1B), while 100/200 µmol/L Sesamin reduced its viability ($p < 0.05$; Fig. 1B). In the NPC C666-1 and HK-1 cells, 20/50/100/200 µmol/L Sesamin significantly weakened the viability ($p < 0.05$; Fig. 1C,D). Therefore, 20 and 50 µmol/L Sesamin were applied for later assays. Besides, according to evaluation results, the inhibited proliferation and promoted apoptosis of Sesamin-induced NPC cells were found (Fig. 1E–H, $p < 0.001$). Collectively, Sesamin may reduce viability and proliferation while inducing the apoptosis of NPC cells.

3.2 Sesamin Inhibited the Migration and Cell Cycle Progression of NPC Cells

As depicted in Fig. 2A,B, the migration rates of both NPC cells C666-1 (Fig. 2A) and HK-1 (Fig. 2B) were diminished by Sesamin ($p < 0.001$). Also, the cell cycle distribution after Sesamin induction (Fig. 2C,D) was confirmed to be decreased in the S phase ($p < 0.05$) and increased in the G0–G1 phase ($p < 0.05$) of the C666-1 cells (Fig. 2C) and HK-1 cells (Fig. 2D), which indicated that Sesamin inhibited the cell cycle progression of NPC cells and hindered the cell cycle in G0–G1 phase.

3.3 Sesamin Influenced the Expressions of Factors Pertinent to Apoptosis/Cell Cycle/Autophagy in NPC Cells

The quantification of apoptosis (cleaved caspase-3 and cleaved PARP1)- and cell cycle (Cyclin B1)-related factors was determined (Fig. 3A–H). The results show that due to Sesamin treatment, cleaved caspase-3/caspase-3 and cleaved PARP1/PARP1 levels in C666-1 cells (Fig. 3A–C) and HK-1 cells (Fig. 3E–G) were up-regulated ($p < 0.01$), while Cyclin B1 level in C666-1 cells (Fig. 3A,D) and HK-1 cells (Fig. 3E,H) were down-regulated ($p < 0.001$). Furthermore, autophagy-related factors (LC3-I, LC3-II, Beclin-1, and P62) were also quantified (Fig. 3I–P). In response to Sesamin treatment, LC3-II/LC3-I ratio and Beclin-1 level in C666-1 cells (Fig. 3I–K) and HK-1 cells (Fig. 3M–O) were elevated ($p < 0.01$), while P62 level in C666-1 cells (Fig. 3I,L) and HK-1 cells (Fig. 3M,P) were deceased ($p < 0.05$). This evidence further confirmed that Sesamin promoted NPC cell apoptosis and autophagy.

3.4 Sesamin Increased ROS Production and Decreased MMP of NPC Cells

Next, the ROS level in NPC cells after Sesamin induction was evaluated (Fig. 4A,B) and the results exhibited that the ROS level in the C666-1 cells (Fig. 4A) and the HK-1 cells (Fig. 4B) was remarkably up-regulated by Sesamin ($p < 0.05$). Besides, as illustrated in Fig. 5A,B, the MMP in the two cells were both decreased after Sesamin treatment ($p < 0.001$). These data proved Sesamin may influence NPC cells by mediating excessive production of ROS.

3.5 Inhibitors of ROS and Autophagy Weakened the Effect of Sesamin on ROS Production, MMP, Proliferation, and Cell Cycle Progression of NPC Cells

To ascertain whether Sesamin influences NPC cells by regulating ROS production and autophagy, the scavenger of ROS (NAC) and the inhibitor of autophagy (3-MA) were used to pre-treat the cells before Sesamin treatment. As depicted in Fig. 6A, the ROS production in HK-1 cells was decreased by 3-MA ($p < 0.01$) and increased by Sesamin ($p < 0.001$), while post-co-treatment with Sesamin and NAC or 3-MA, the effect of Sesamin on ROS production was weakened by NAC or 3-MA ($p < 0.05$). Meanwhile, the influence of Sesamin on decreasing MMP of HK-1 cells was also attenuated by NAC and 3-MA, respectively (Fig. 6B, $p < 0.001$). Furthermore, the proliferation (Fig. 7A) and cell cycle distribution (Fig. 7B) were determined. The inhibiting role of Sesamin in HK-1 cell proliferation was weakened by both NAC and 3-MA (Fig. 7A, $p < 0.01$). As for the cell cycle distribution (Fig. 7B), NAC and 3-MA increased the S phase level ($p < 0.05$), while Sesamin decreased the S phase and G2 phase level ($p < 0.01$) and increased the G0–G1 phase level ($p < 0.001$) of the cells. Notably, after treatment with Sesamin and NAC or Sesamin and 3-MA, the influence of Sesamin on the cell cycle distribution was counteracted by NAC or 3-MA ($p < 0.05$). All the discoveries indicated that Sesamin mediated proliferation and cell cycle distribution of NPC cells by regulating ROS production and autophagy.

3.6 Inhibitors of ROS and Autophagy Weakened the Role of Sesamin in the Apoptosis and Expressions of Apoptosis-/Autophagy-related Factors in NPC Cells

In addition, HK-1 cell apoptosis was determined (Fig. 8A) and the results showed that Sesamin-induced changes in apoptosis were counteracted by NAC and 3-MA ($p < 0.001$). Meanwhile, NAC and 3-MA abrogated Sesamin-induced up-regulated cleaved caspase-3/caspase-3 (Fig. 8B,C, $p < 0.01$) and cleaved PARP1/PARP1 (Fig. 8B,D, $p < 0.05$) and down-regulated Cyclin B1 (Fig. 8B,E, $p < 0.001$). As for the expressions of autophagy-related factors (Fig. 8F–I), LC3-II/LC3-I ratio (Fig. 8F,G) was decreased by NAC ($p < 0.001$) or 3-MA ($p < 0.001$), which also further weakened the promoting effect of Sesamin on LC3-II/LC3-I ratio ($p < 0.01$). Sesamin-induced up-regulation in Beclin-1 (Fig. 8F,H, $p < 0.001$)

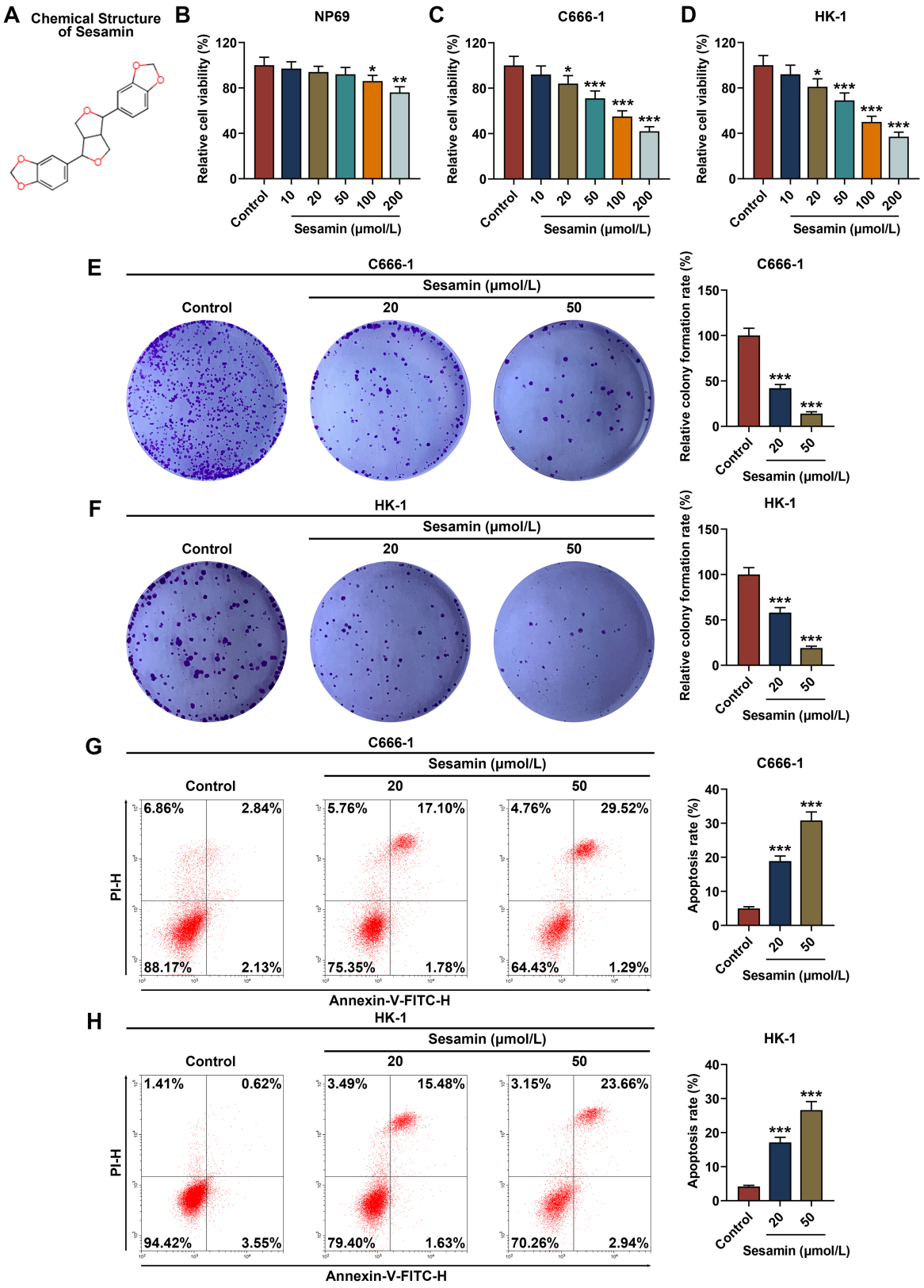

Fig. 1. Sesamin reduced viability and proliferation while enhancing apoptosis of NPC cells. (A) The chemical structure of Sesamin. (B–D) Viability of NP69 cells (B), C666-1 cells (C), and HK-1 cells (D) after Sesamin treatment (MTT assay). (E,F) Proliferation of C666-1 cells (E) and HK-1 cells (F) after Sesamin treatment (colony formation assay). (G,H) Apoptosis of C666-1 cells (G) and HK-1 cells (H) after Sesamin treatment (flow cytometry). ($^{*}p < 0.05$, $^{**}p < 0.01$,$^{***}p < 0.001$, vs. Control, n = 3). NPC, nasopharyngeal carcinoma; MTT, methylthiazolyldiphenyl-tetrazolium bromide.

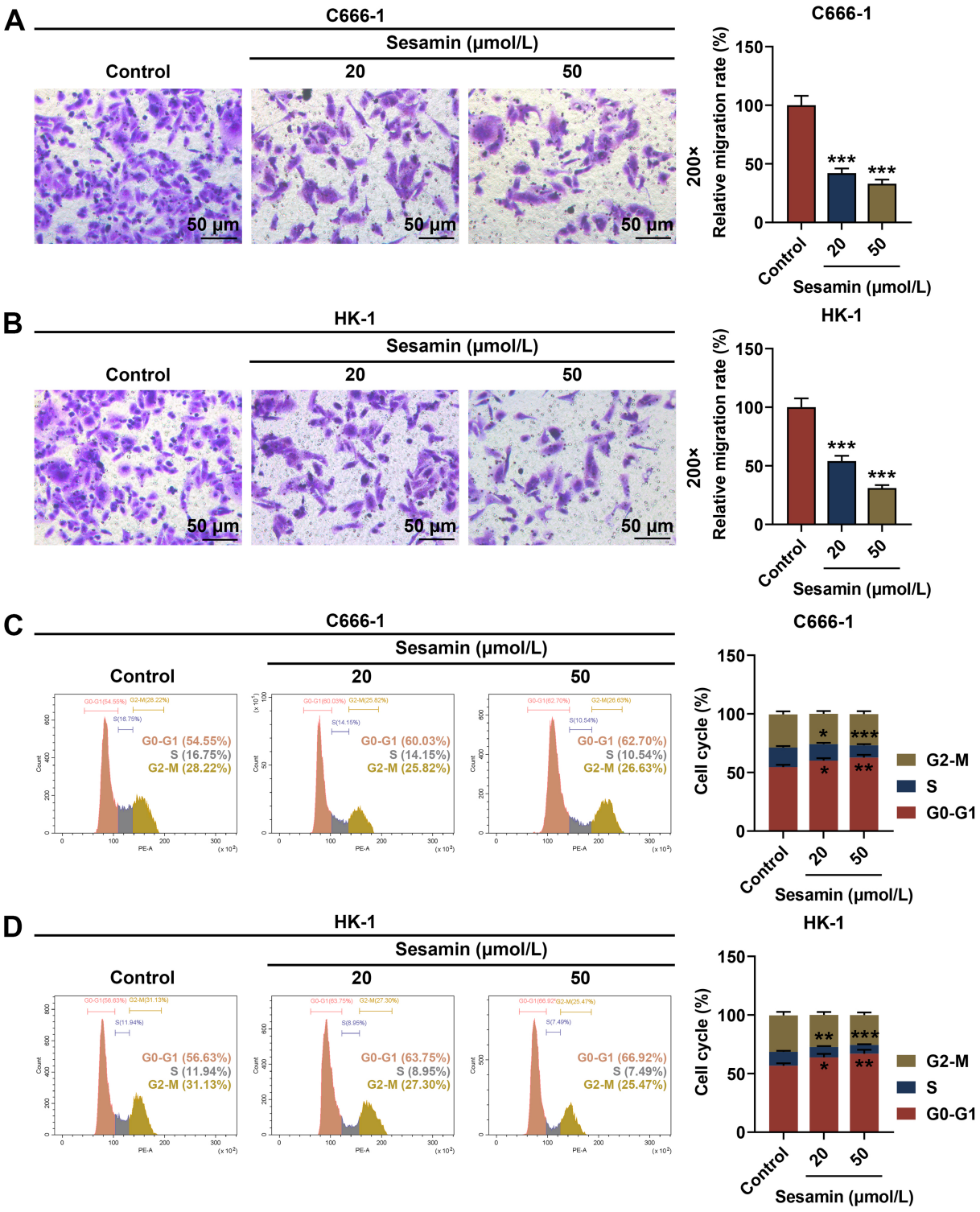

Fig. 2. Sesamin inhibited the migration and cell cycle progression of NPC cells. (A,B) Migration of C666-1 cells (A) and HK-1 cells (B) after Sesamin treatment (transwell assay). Scale bars, 50 μm. (C,D) Cell cycle distribution of C666-1 cells (C) and HK-1 cells (D) after Sesamin treatment (flow cytometry). ($^{*}p < 0.05$, $^{**}p < 0.01$, $^{***}p < 0.001$, vs. Control, n = 3). NPC, nasopharyngeal carcinoma.

and down-regulation in P62 (Fig. 8F,I, $p < 0.001$) were all weakened by NAC or 3-MA ($p < 0.01$). All the findings proved that Sesamin regulated NPC cell apoptosis by impacting apoptosis/autophagy-related factors.

3.7 Sesamin Down-Regulated Ki-67 and Up-Regulated Cleaved Caspase-3 in NPC Tumors, as well as Inhibited NPC Growth In Vivo

Finally, to further verify the influence of Sesamin *in vivo*, the xenografted tumor mice model was estab-

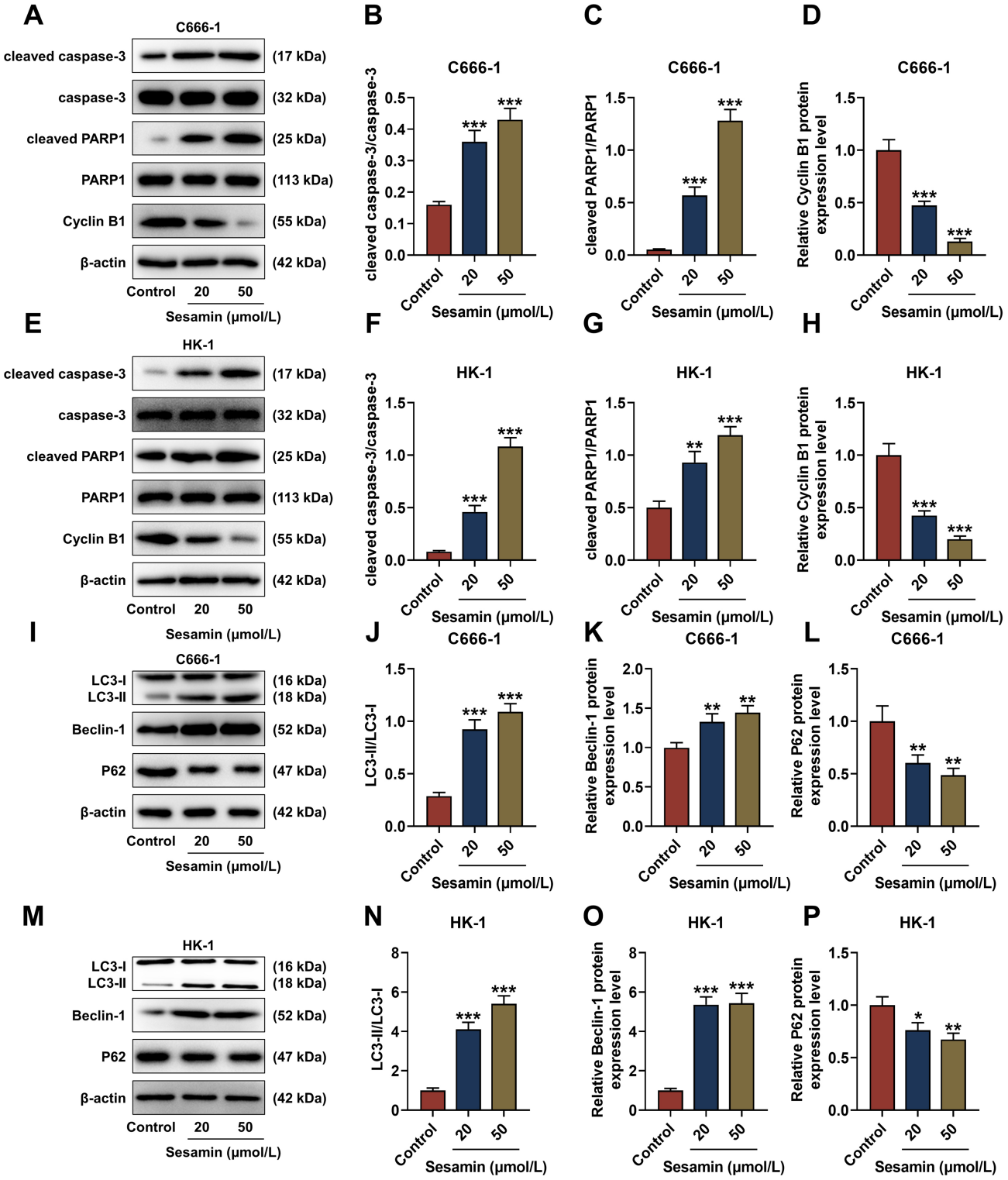

Fig. 3. Sesamin influenced expressions of factors related to apoptosis/cell cycle/autophagy in NPC cells. (A–H) Expressions of apoptosis-related (cleaved caspase-3, caspase-3, cleaved PARP1, and PARP1) and cell cycle-related (Cyclin B1) factors in C666-1 cells (A–D) and HK-1 cells (E–H) after Sesamin treatment (Western blot assay). (I–P) Expressions of autophagy-related factors (LC3-I, LC3-II, Beclin-1, and P62) in C666-1 cells (I–L) and HK-1 cells (M–P) after Sesamin treatment (Western blot assay). β-actin acted as an internal control. ($^{*}p < 0.05$, $^{**}p < 0.01$, $^{***}p < 0.001$, vs. Control, n = 3). NPC, nasopharyngeal carcinoma; PARP1, cleaved poly (ADP-ribose) polymerase 1.

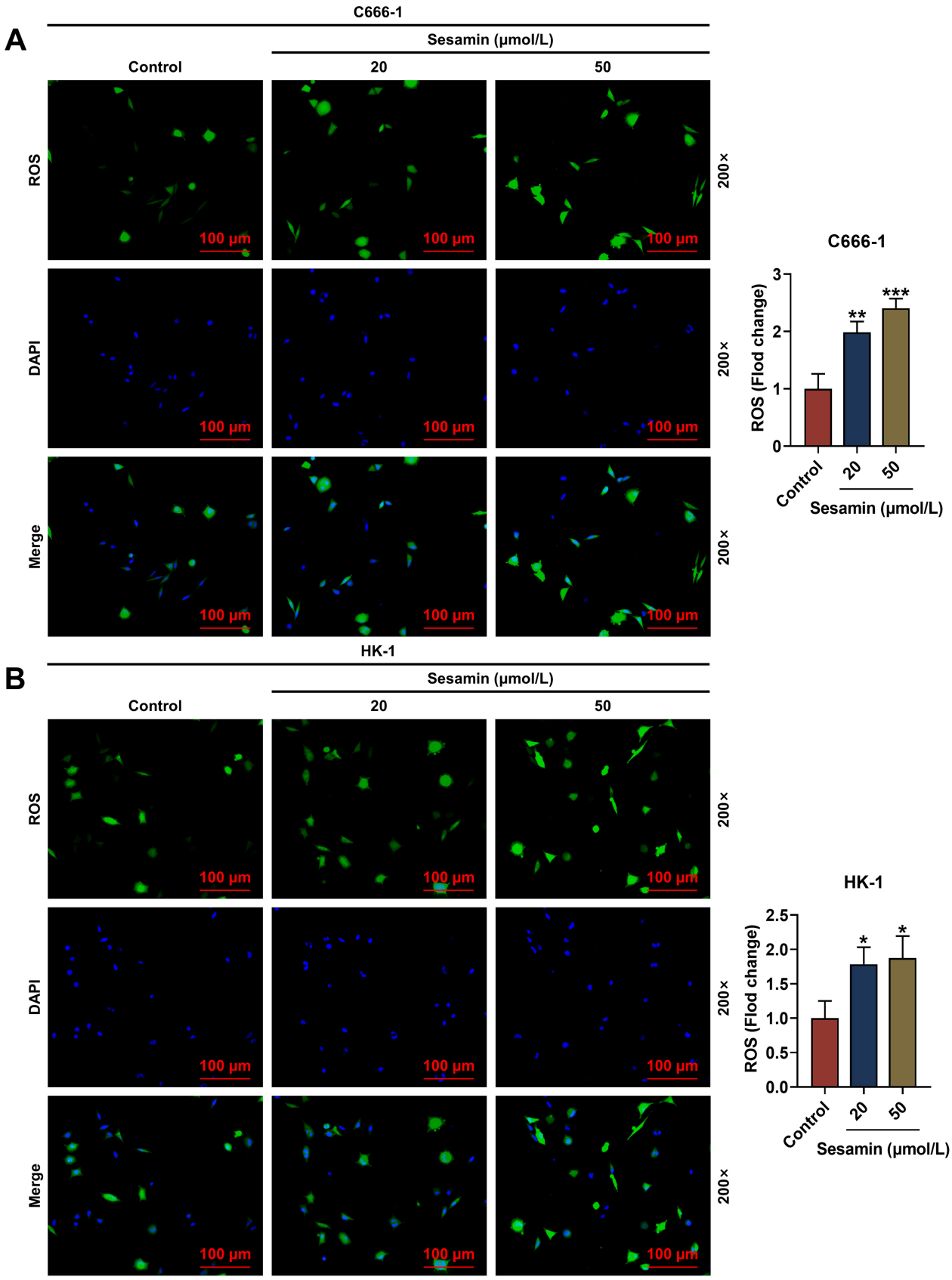

Fig. 4. Sesamin increased ROS production. (A,B) The ROS level in C666-1 cells (A) and HK-1 cells (B) after Sesamin treatment (DCFH-DA staining). Scale bars, 100 μm. ($^{*}p < 0.05$, $^{**}p < 0.01$, $^{***}p < 0.001$, vs. Control, n = 3). ROS, reactive oxygen species; DCFH-DA, dichlorodihydrofluorescein diacetate.

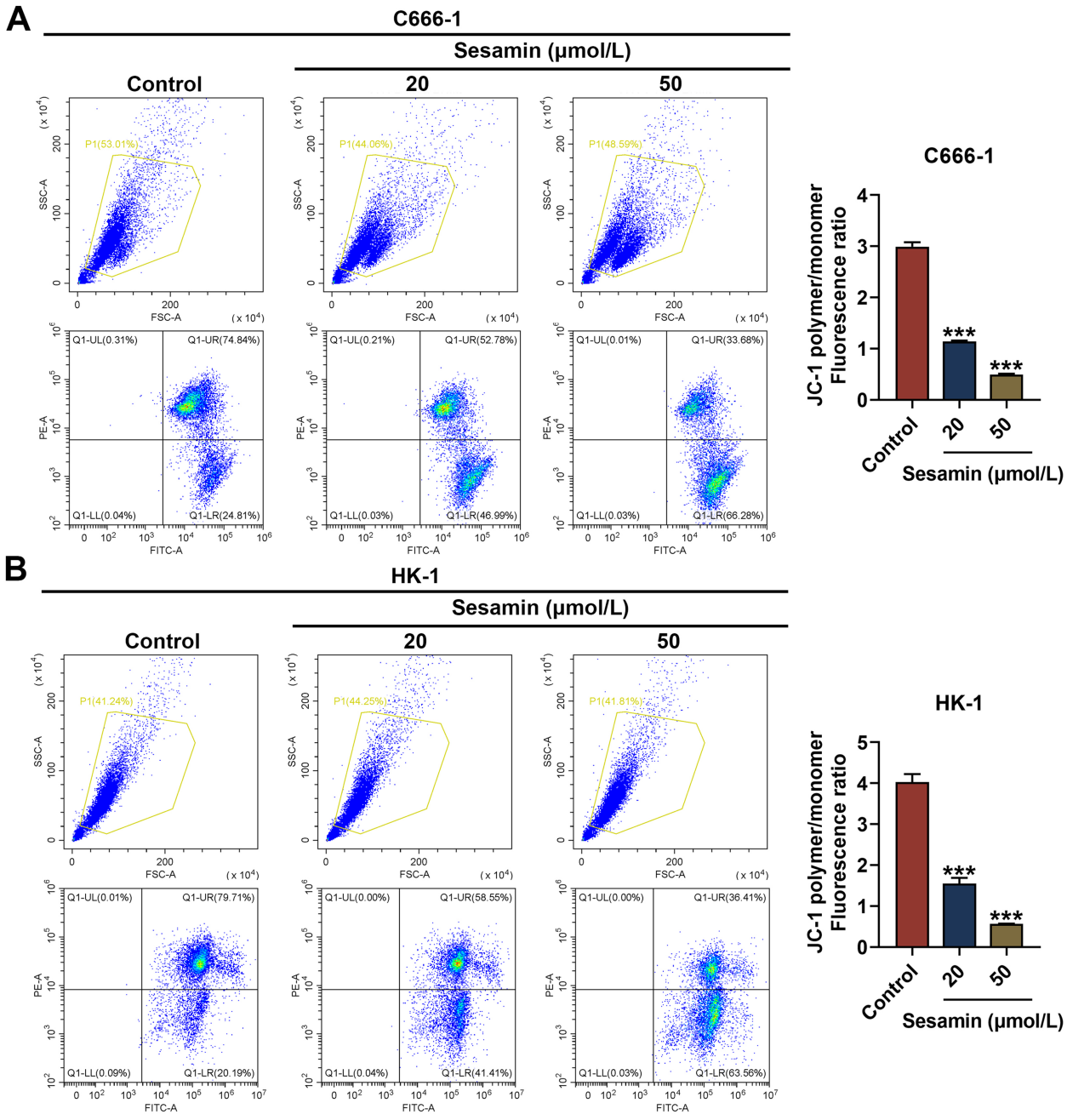

Fig. 5. Sesamin decreased MMP of NPC cells. (A,B) The mitochondrial membrane potential of C666-1 cells (A) and HK-1 cells (B) after Sesamin treatment (flow cytometry). ($^{***}p < 0.001$, vs. Control, n = 3). MMP, mitochondrial membrane potential; NPC, nasopharyngeal carcinoma.

lished and treated with Sesamin. As shown in Fig. 9A, Sesamin treatment significantly inhibited the increases in tumor volume ($p < 0.001$, Fig. 9A) and weight ($p < 0.001$, Fig. 9D) without side effects on mouse body weight (Fig. 9B). Fig. 9C displayed solid tumor. In addition, Sesamin treatment visibly decreased the Ki-67 level ($p < 0.05$, Fig. 9E,G) and augmented cleaved caspase-3 level ($p < 0.05$, Fig. 9F,H) in the tumor tissues. All these discoveries further proved that Sesamin promoted the apoptosis of NPC cells and inhibited NPC growth.

4. Discussion

The powerful anti-tumor effect of Sesamin has been previously reported [17] in many cancers except NPC. Herein, for the first time, we discovered that Sesamin inhibited the proliferation, migration, and cell cycle progression, while inducing apoptosis of NPC cells, which indicated that Sesamin might have an anti-tumor effect on NPC. Considering that the basis of cancer development is enhanced proliferation and suppressed apoptosis of cancer cells [24], and that proliferation is contingent upon cell cycle distribution

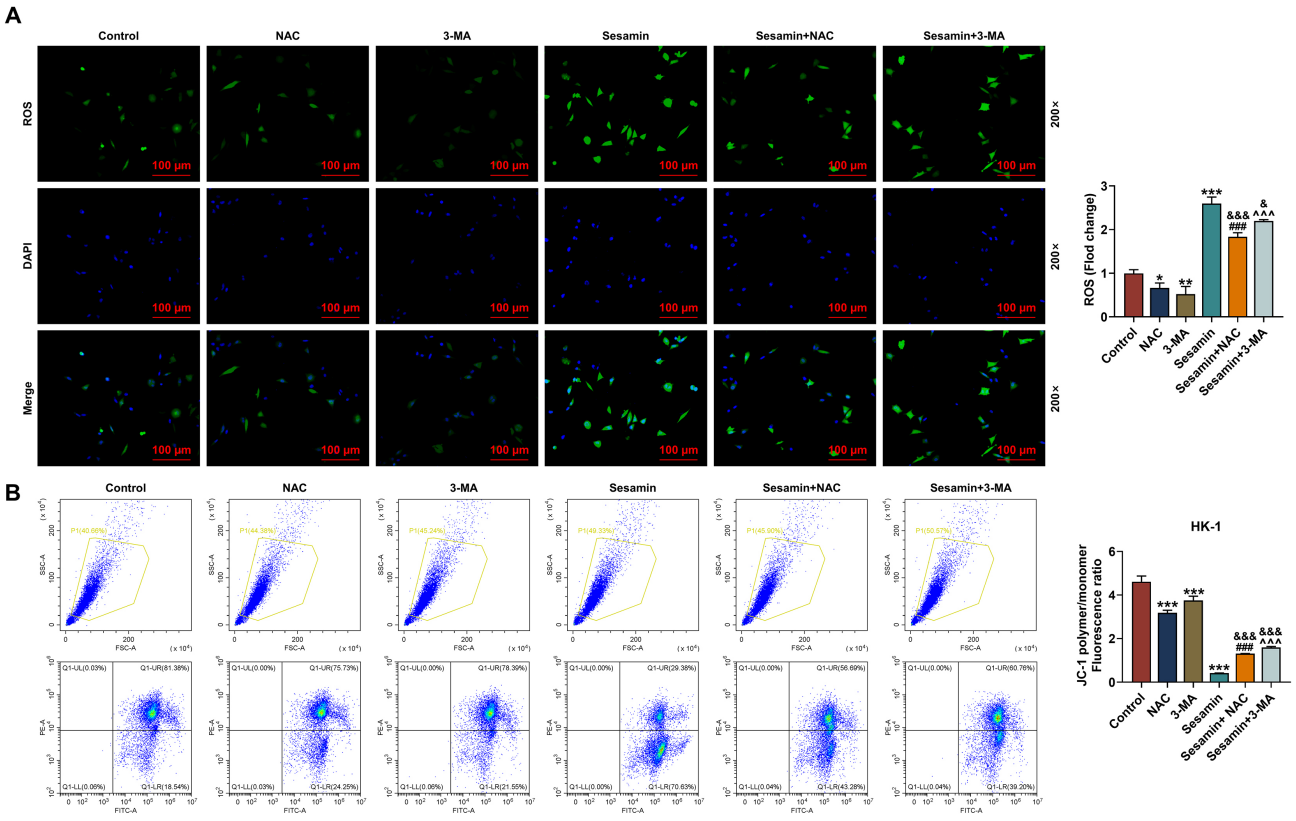

Fig. 6. Inhibitors of ROS and autophagy neutralized the effect of Sesamin on ROS production, and MMP of the NPC cells. (A) The ROS level in HK-1 cells after being co-treated with Sesamin and NAC or 3-MA (DCFH-DA staining). Scale bars, 100 μm. (B) Mitochondrial membrane potential of HK-1 cells after being co-treated with Sesamin and NAC or Sesamin and 3-MA (flow cytometry). ($^{*}p < 0.05$, $^{**}p < 0.01$, $^{***}p < 0.001$, vs. Control; $^{\#\#\#}p < 0.001$, vs. NAC; $^{\wedge\wedge\wedge}p < 0.001$, vs. 3-MA; $^{\&}p < 0.05$, $^{\&\&\&}p < 0.001$, vs. Sesamin, n = 3). NPC, nasopharyngeal carcinoma; ROS, reactive oxygen species; NAC, n-acetyl-L-cysteine.

of cancer cells [24–27], we conducted an assessment on cell cycle-associated factors. The S phase is a stage where DNA and histone synthesis occur before cell division [28]. Besides, Cyclin B1, one of the cell cycle regulation factors, starts to be expressed in the S phase [29,30]. A previous study showed Sesamin stimulated cell cycle arrest and apoptosis in human colorectal cancer cells [31]. Our results proved that Sesamin diminished Cyclin B1 level, and dampened the cell cycle progression of NPC cells.

Besides, apoptosis is closely associated with DNA damage. PARP, regarded as a DNA damage receptor, can be activated (cleaved PARP) to be involved in the repair of cell injury, especially during stress conditions including cell apoptosis [32,33]. PARP1 is a substrate of caspase-3 [34]. Once activated (cleaved caspase-3), caspase-3 is the final executor of cell apoptosis [24]. Therefore, cleaved caspase-3 and cleaved PARP levels can affect the apoptosis level in cells. Herein, Sesamin up-regulated cleaved caspase-3 and cleaved PARP in NPC cells. Moreover, apoptosis is mainly mediated by the mitochondrial pathway (Bcl-2 family/caspase 9/caspase 3), which is characterized by the continuous activation of caspase [35]. Apoptosis enhances mitochondrial membrane permeability and attenuates the transmembrane MMP [36]. In the mitochondrial apoptosis pathway, the reduction of MMP promotes the release of cytochrome c (Cyt c) from the mitochondria into the cytoplasm, activating caspase-3 [37]. Furthermore, ROS is essential in tumorigenesis, and ROS accumulation directly causes DNA damage [38–40]. Therefore, ROS both participates in apoptosis and autophagy. Excessive ROS also induces cell cycle arrest [38]. Interestingly, ROS production was boosted by Sesamin treatment. Given that ROS is generated in mitochondria, which are also the main targets of ROS, ROS production leads to mitochondrial damage manifested by a decrease in cell MMP [41]. In this study, we found that Sesamin reduced the MMP of NPC cells and promoted ROS production in NPC cells.

Although apoptosis and autophagy are both programmed cell death mechanisms, autophagy also can serve as an alternative mechanism for cell death especially when apoptosis is defective [15,38]. Given the current challenges in cancer treatment and possible cancer resistance to apoptosis, targeting autophagy presents a promising strategy to induce cancer cell death [15]. Sesamin may alleviate asthma airway inflammation by inhibiting mitophagy and mitochondrial apoptosis [42]. Therefore, we hypoth-

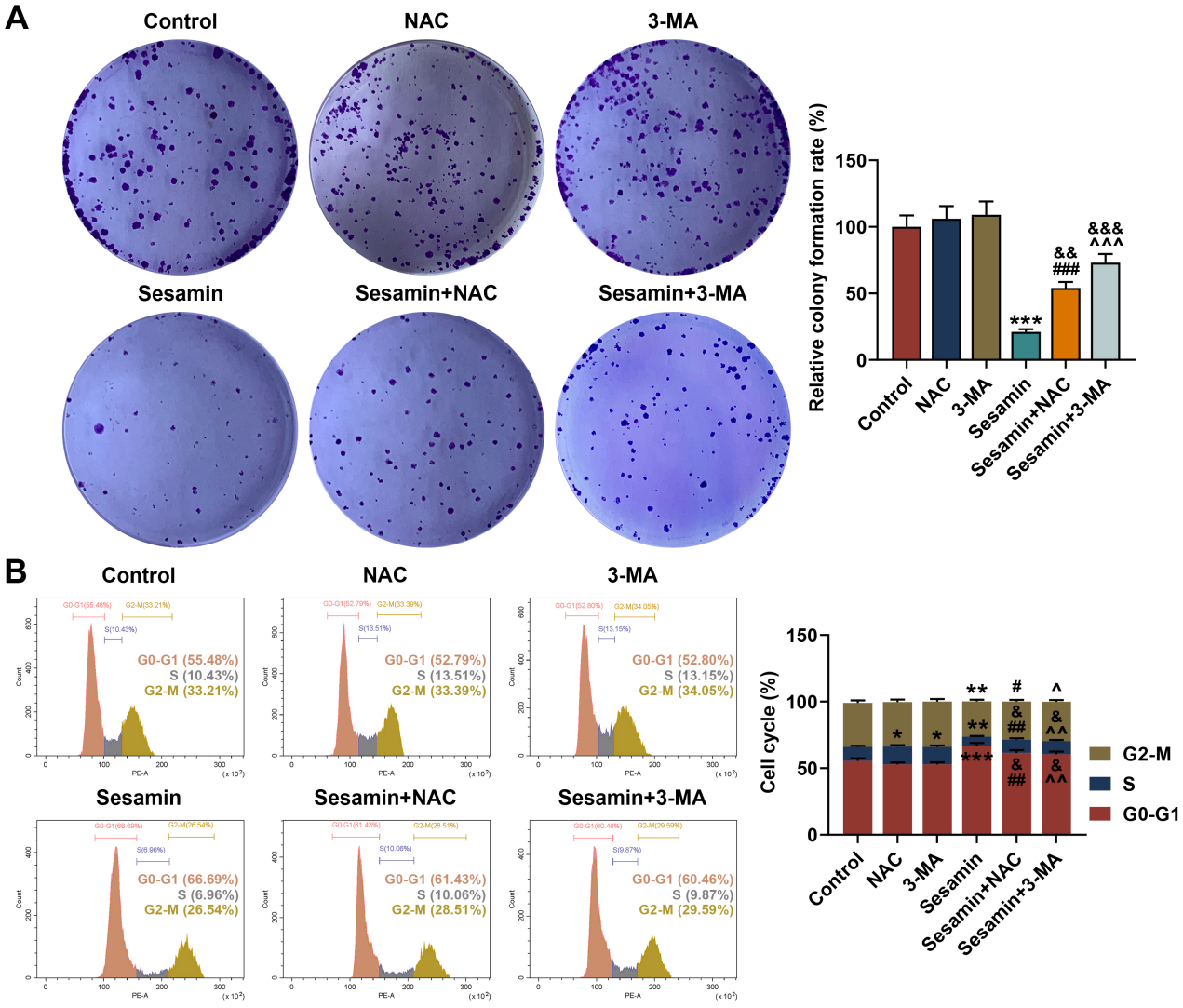

Fig. 7. Inhibitors of ROS and autophagy neutralized the effect of Sesamin on proliferation, and cell cycle progression of the NPC cells. (A) Proliferation of HK-1 cells after being co-treated with Sesamin and NAC or 3-MA (colony formation assay). (B) Cell cycle distribution of HK-1 cells after being co-treated with Sesamin and NAC or 3-MA (flow cytometry). ($^{*}p < 0.05$, $^{**}p < 0.01$, $^{***}p < 0.001$, vs. Control; $^{\#}p < 0.05$, $^{\#\#}p < 0.01$, $^{\#\#\#}p < 0.001$, vs. NAC; $^{\wedge}p < 0.05$, $^{\wedge\wedge}p < 0.01$, $^{\wedge\wedge\wedge}p < 0.001$, vs. 3-MA; $^{\&}p < 0.05$, $^{\&\&}p < 0.01$, $^{\&\&\&}p < 0.001$, vs. Sesamin, n = 3). NPC, nasopharyngeal carcinoma; ROS, reactive oxygen species.

esized that Sesamin may impact NPC cells by promoting autophagy. To investigate whether Sesamin can promote autophagy in NPC cells, the autophagy-related factors were evaluated. LC3 is a widely accepted autophagy marker due to its ability to transform into LC3-II during autophagy, and Beclin-1 is the upstream factor essential for autophagosome formation [38]. Herein, LC3-II/LC3-I ratio and Beclin-1 level were both elevated by Sesamin treatment, hinting that Sesamin promoted autophagy in NPC cells.

To further confirm our hypothesis, we co-treated NPC cells with NAC/3-MA alongside Sesamin. To our delight, the data revealed the impacts of Sesamin on the proliferation, cell cycle distribution, apoptosis, ROS production, MMP, and expressions of related factors in NPC cells were weakened by NAC/3-MA, which supported our hypothesis. In addition, in the xenografted tumor mice, we further discovered that Sesamin inhibited the growth of NPC tumors and promoted apoptosis of NPC tumor cells, which further verified the anti-tumor effect of Sesamin on NPC *in vivo*. However, the ROS level was not measured in animal experiments, which will be performed in the future. Moreover, different NPC cells have different characteristics and may have different sensitivity to Sesamin. Therefore, it is necessary to further explore the basic principle governing different cell sensitivity to Sesamin in the future.

5. Conclusion

In a word, this research discovers that Sesamin inhibits proliferation and promotes apoptosis of NPC both *in vitro* and *in vivo* through stimulating autophagy and ROS pro-

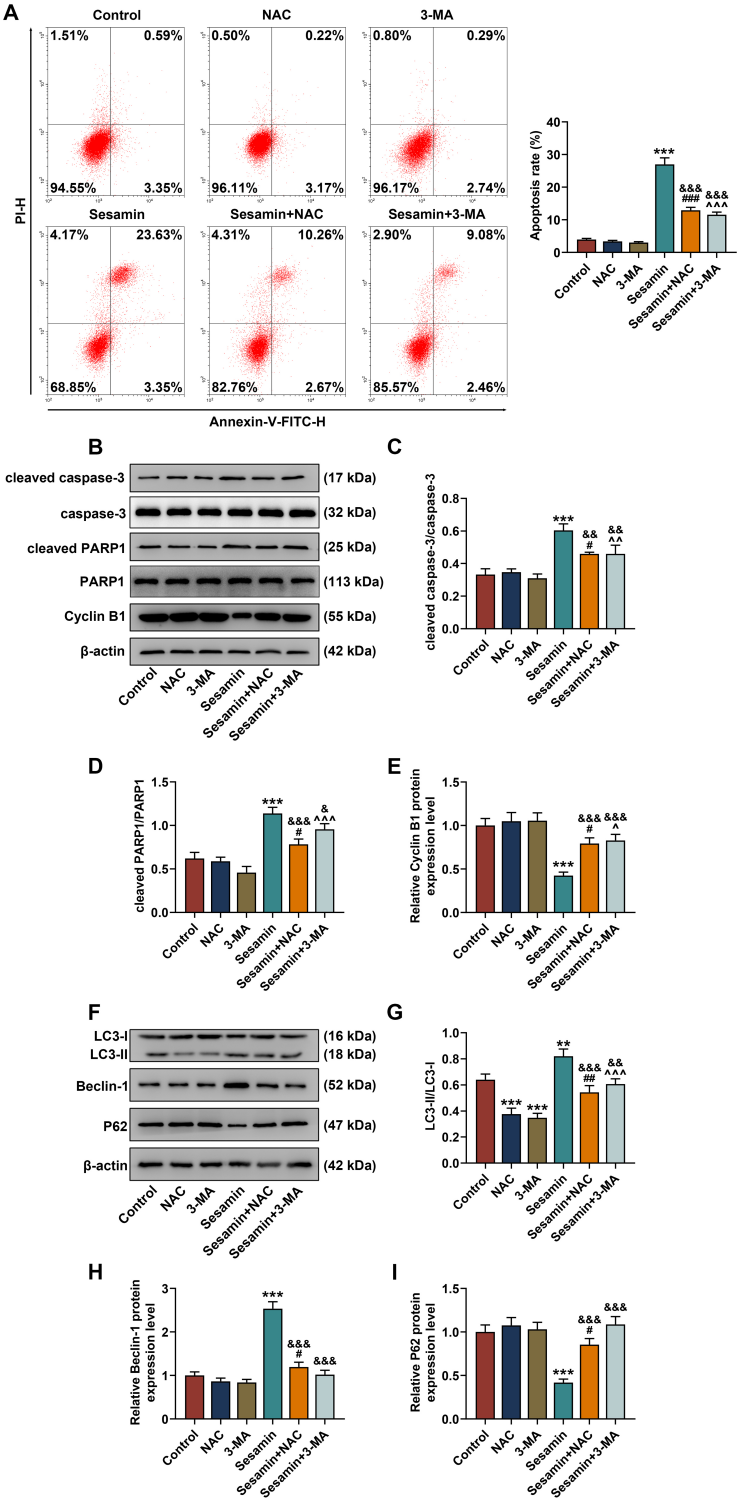

Fig. 8. Inhibitors of ROS and autophagy abrogated Sesamin-triggered changes in the apoptosis and expressions of apoptosis/autophagy-related factors in NPC cells. (A) HK-1 cell apoptosis after being co-treated with Sesamin and NAC or 3-MA (flow cytometry). (B–E) The expressions of apoptosis- (cleaved caspase-3/caspase-3 and cleaved PARP1/PARP1) and cell cycle (Cycle B1)-related factors in HK-1 cells after being co-treated with Sesamin and NAC or 3-MA (Western blot assays). (F–I) The expressions of autophagy-related factors (LC3-I, LC3-II, Beclin-1, and P62) in HK-1 cells after being co-treated with Sesamin and NAC or 3-MA (Western blot assay). β-actin functioned as an internal control in Western blot assays. ($^{**}p < 0.01$, $^{***}p < 0.001$, vs. Control; $^{\#}p < 0.05$, $^{\#\#}p < 0.01$, $^{\#\#\#}p < 0.001$, vs. NAC; $^{\wedge}p < 0.05$, $^{\wedge\wedge}p < 0.01$, $^{\wedge\wedge\wedge}p < 0.001$, vs. 3-MA; $^{\&}p < 0.05$, $^{\&\&}p < 0.01$, $^{\&\&\&}p < 0.001$, vs. Sesamin, n = 3). NPC, nasopharyngeal carcinoma.

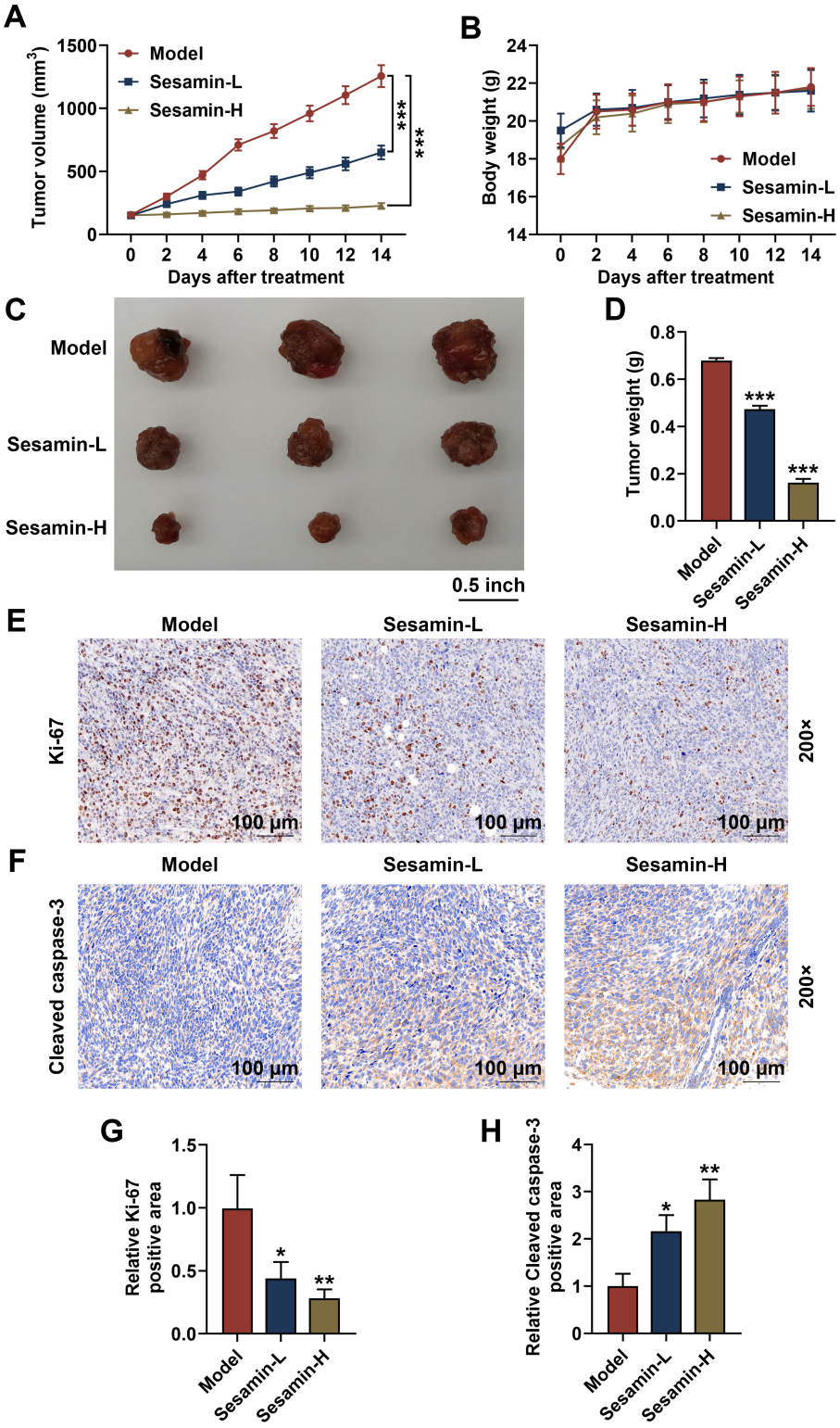

Fig. 9. Sesamin down-regulated Ki-67 and up-regulated cleaved caspase-3 in NPC tumors, as well as inhibited the growth of NPC *in vivo*. (A) Tumor volume subcutaneously growing in nude mice on days 0, 2, 4, 6, 8, 10, 12, or 14, n = 6. (B) The body weight of the mice on days 0, 2, 4, 6, 8, 10, 12, or 14 when tumor subcutaneously grown in nude mice, n = 6. (C) Pictures of xenografted tumor subcutaneously grown in nude mice for 14 days, n = 3. (D) Tumor weight after the tumor subcutaneously grown in nude mice for 14 days, n = 3. (E,G) Ki-67 expression in the tumor tissues (immunohistochemical analysis). Scale bars, 100 μm. (F,H) Cleaved caspase-3 expression in the tumor tissues (immunohistochemical analysis). ($^{*}p < 0.05$, $^{**}p < 0.01$, $^{***}p < 0.001$, vs. Model, n = 3). Scale bars, 100 μm. NPC, nasopharyngeal carcinoma.

duction. Our findings provide novel theoretical guidance for the study of Sesamin and may pave the way for innovative therapeutic strategies against NPC.

Availability of Data and Materials

The analyzed data sets generated during the study are available from the corresponding author on reasonable request.

Author Contributions

Substantial contributions to conception and design: DQA. Data acquisition, data analysis and interpretation: XYJ, YCY. Drafting the article or critically revising it for important intellectual content: All authtors. Final approval of the version to be published: All authors. Agreement to be accountable for all aspects of the work in ensuring that questions related to the accuracy or integrity of the work are appropriately investigated and resolved: All authors.

Ethics Approval and Consent to Participate

All experiments involved in animals in this study were ratified by the Committee of Zhejiang Baiyue Biotech Co., Ltd. for Experimental Animals Welfare (No. ZJBYLA-IACUC-20231201). The experimental guidelines we follow for animal experiments are: Institutional Animal Care and Use Committee ethical guidelines.

Acknowledgment

Not applicable.

Funding

This work was supported by the National Natural Science Foundation of China (grant no. 81970864); the Chongqing Middle and Youth Medical High-end Talent Studio Project (grant no. Yu Wei (2018) No 2) and the Chongqing Talents Project (grant no. Yu Wei (2021)).

Conflict of Interest

The authors declare no conflict of interest.

References

[1] Lee HM, Okuda KS, González FE, Patel V. Current Perspectives on Nasopharyngeal Carcinoma. Advances in Experimental Medicine and Biology. 2019; 1164: 11–34. https://doi.org/10.1007/978-3-030-22254-3_2.

[2] Guo R, Mao YP, Tang LL, Chen L, Sun Y, Ma J. The evolution of nasopharyngeal carcinoma staging. The British Journal of Radiology. 2019; 92: 20190244. https://doi.org/10.1259/bjr.20190244.

[3] Chen YP, Chan ATC, Le QT, Blanchard P, Sun Y, Ma J. Nasopharyngeal carcinoma. Lancet (London, England). 2019; 394: 64–80. https://doi.org/10.1016/S0140-6736(19)30956-0.

[4] Zhang Q, Wu G, Yang Q, Dai G, Li T, Chen P, *et al*. Survival rate prediction of nasopharyngeal carcinoma patients based on MRI and gene expression using a deep neural network. Cancer Science. 2023; 114: 1596–1605. https://doi.org/10.1111/cas.15704.

[5] Huang H, Yao Y, Deng X, Huang Z, Chen Y, Wang Z, *et al*. Immunotherapy for nasopharyngeal carcinoma: Current status and prospects (Review). International Journal of Oncology. 2023; 63: 97. https://doi.org/10.3892/ijo.2023.5545.

[6] Chen E, Huang J, Chen M, Wu J, Ouyang P, Wang X, *et al*. FLI1 regulates radiotherapy resistance in nasopharyngeal carcinoma through TIE1-mediated PI3K/AKT signaling pathway. Journal of Translational Medicine. 2023; 21: 134. https://doi.org/10.1186/s12967-023-03986-y.

[7] Spradlin JN, Hu X, Ward CC, Brittain SM, Jones MD, Ou L, *et al*. Harnessing the anti-cancer natural product nimbolide for targeted protein degradation. Nature Chemical Biology. 2019; 15: 747–755. https://doi.org/10.1038/s41589-019-0304-8.

[8] Zeng Y, Ma J, Xu L, Wu D. Natural Product Gossypol and its Derivatives in Precision Cancer Medicine. Current Medicinal Chemistry. 2019; 26: 1849–1873. https://doi.org/10.2174/0929867324666170523123655.

[9] Chen L, Chan LS, Lung HL, Yip TTC, Ngan RKC, Wong JWC, *et al*. Crucifera sulforaphane (SFN) inhibits the growth of nasopharyngeal carcinoma through DNA methyltransferase 1 (DNMT1)/Wnt inhibitory factor 1 (WIF1) axis. Phytomedicine: International Journal of Phytotherapy and Phytopharmacology. 2019; 63: 153058. https://doi.org/10.1016/j.phymed.2019.153058.

[10] Zhou C, Tang X, Xu J, Wang J, Yang Y, Chen Y, *et al*. Opening of the CLC-3 chloride channel induced by dihydroartemisinin contributed to early apoptotic events in human poorly differentiated nasopharyngeal carcinoma cells. Journal of Cellular Biochemistry. 2018; 119: 9560–9572. https://doi.org/10.1002/jcb.27274.

[11] Ong CS, Zhou J, Ong CN, Shen HM. Luteolin induces G1 arrest in human nasopharyngeal carcinoma cells via the Akt-GSK-3β-Cyclin D1 pathway. Cancer Letters. 2010; 298: 167–175. https://doi.org/10.1016/j.canlet.2010.07.001.

[12] Kumano T, Fujiki E, Hashimoto Y, Kobayashi M. Discovery of a sesamin-metabolizing microorganism and a new enzyme. Proceedings of the National Academy of Sciences of the United States of America. 2016; 113: 9087–9092. https://doi.org/10.1073/pnas.1605050113.

[13] Farbood Y, Ghaderi S, Rashno M, Khoshnam SE, Khorsandi L, Sarkaki A, *et al*. Sesamin: A promising protective agent against diabetes-associated cognitive decline in rats. Life Sciences. 2019; 230: 169–177. https://doi.org/10.1016/j.lfs.2019.05.071.

[14] Lin TY, Wu PY, Hou CW, Chien TY, Chang QX, Wen KC, *et al*. Protective Effects of Sesamin against UVB-Induced Skin Inflammation and Photodamage In Vitro and In Vivo. Biomolecules. 2019; 9: 479. https://doi.org/10.3390/biom9090479.

[15] Dou H, Yang S, Hu Y, Xu D, Liu L, Li X. Sesamin induces ER stress-mediated apoptosis and activates autophagy in cervical cancer cells. Life Sciences. 2018; 200: 87–93. https://doi.org/10.1016/j.lfs.2018.03.003.

[16] Tai TS, Tien N, Shen HY, Chu FY, Wang CCN, Lu CH, *et al*. Sesamin, a Naturally Occurring Lignan, Inhibits Ligand-Induced Lipogenesis through Interaction with Liver X Receptor Alpha (LXRα) and Pregnane X Receptor (PXR). Evidence-based Complementary and Alternative Medicine: ECAM. 2019; 2019: 9401648. https://doi.org/10.1155/2019/9401648.

[17] Majdalawieh AF, Massri M, Nasrallah GK. A comprehensive review on the anti-cancer properties and mechanisms of action of sesamin, a lignan in sesame seeds (Sesamum indicum). European Journal of Pharmacology. 2017; 815: 512–521. https://doi.org/10.1016/j.ejphar.2017.10.020.

[18] Chen Y, Li H, Zhang W, Qi W, Lu C, Huang H, *et al*. Sesamin suppresses NSCLC cell proliferation and induces apoptosis via

Akt/p53 pathway. Toxicology and Applied Pharmacology. 2020; 387: 114848. https://doi.org/10.1016/j.taap.2019.114848.

[19] Kongtawelert P, Wudtiwai B, Shwe TH, Pothacharoen P, Phitak T. Inhibition of programmed death ligand 1 (PD-L1) expression in breast cancer cells by sesamin. International Immunopharmacology. 2020; 86: 106759. https://doi.org/10.1016/j.intimp.2020.106759.

[20] Qin ZQ, Li QG, Yi H, Lu SS, Huang W, Rong ZX, *et al*. Heterozygous p53-R280T Mutation Enhances the Oncogenicity of NPC Cells Through Activating PI3K-Akt Signaling Pathway. Frontiers in Oncology. 2020; 10: 104. https://doi.org/10.3389/fonc.2020.00104.

[21] Wang Z, Mao JW, Liu GY, Wang FG, Ju ZS, Zhou D, *et al*. MicroRNA-372 enhances radiosensitivity while inhibiting cell invasion and metastasis in nasopharyngeal carcinoma through activating the PBK-dependent p53 signaling pathway. Cancer Medicine. 2019; 8: 712–728. https://doi.org/10.1002/cam4.1924.

[22] Johnson D, Ma BBY. Targeting the PD-1/ PD-L1 interaction in nasopharyngeal carcinoma. Oral Oncology. 2021; 113: 105127. https://doi.org/10.1016/j.oraloncology.2020.105127.

[23] Tan GX, Wang XN, Tang YY, Cen WJ, Li ZH, Wang GC, *et al*. PP-22 promotes autophagy and apoptosis in the nasopharyngeal carcinoma cell line CNE-2 by inducing endoplasmic reticulum stress, downregulating STAT3 signaling, and modulating the MAPK pathway. Journal of Cellular Physiology. 2019; 234: 2618–2630. https://doi.org/10.1002/jcp.27076.

[24] Yang H, Liu JX, Shang HX, Lin S, Zhao JY, Lin JM. Qingjie Fuzheng granules inhibit colorectal cancer cell growth by the PI3K/AKT and ERK pathways. World Journal of Gastrointestinal Oncology. 2019; 11: 377–392. https://doi.org/10.4251/wjgo.v11.i5.377.

[25] Liu L, Michowski W, Kolodziejczyk A, Sicinski P. The cell cycle in stem cell proliferation, pluripotency and differentiation. Nature Cell Biology. 2019; 21: 1060–1067. https://doi.org/10.1038/s41556-019-0384-4.

[26] Mohamed TMA, Ang YS, Radzinsky E, Zhou P, Huang Y, Elfenbein A, *et al*. Regulation of Cell Cycle to Stimulate Adult Cardiomyocyte Proliferation and Cardiac Regeneration. Cell. 2018; 173: 104–116.e12. https://doi.org/10.1016/j.cell.2018.02.014.

[27] Ponnusamy M, Li PF, Wang K. Understanding cardiomyocyte proliferation: an insight into cell cycle activity. Cellular and Molecular Life Sciences: CMLS. 2017; 74: 1019–1034. https://doi.org/10.1007/s00018-016-2375-y.

[28] Pan Z, Luo Y, Xia Y, Zhang X, Qin Y, Liu W, *et al*. Cinobufagin induces cell cycle arrest at the S phase and promotes apoptosis in nasopharyngeal carcinoma cells. Biomedicine & Pharmacotherapy = Biomedecine & Pharmacotherapie. 2020; 122: 109763. https://doi.org/10.1016/j.biopha.2019.109763.

[29] Schnittger A, De Veylder L. The Dual Face of Cyclin B1. Trends in Plant Science. 2018; 23: 475–478. https://doi.org/10.1016/j.tplants.2018.03.015.

[30] Xie B, Wang S, Jiang N, Li JJ. Cyclin B1/CDK1-regulated mitochondrial bioenergetics in cell cycle progression and tumor resistance. Cancer Letters. 2019; 443: 56–66. https://doi.org/10.1016/j.canlet.2018.11.019.

[31] Wang X, Qiao J, Zou C, Zhao Y, Huang Y. Sesamin induces cell cycle arrest and apoptosis through p38/C-Jun N-terminal kinase mitogen-activated protein kinase pathways in human colorectal cancer cells. Anti-cancer Drugs. 2021; 32: 248–256. https://doi.org/10.1097/CAD.0000000000001031.

[32] Mateo J, Lord CJ, Serra V, Tutt A, Balmaña J, Castroviejo-Bermejo M, *et al*. A decade of clinical development of PARP inhibitors in perspective. Annals of Oncology: Official Journal of the European Society for Medical Oncology. 2019; 30: 1437–1447. https://doi.org/10.1093/annonc/mdz192.

[33] Sachdev E, Tabatabai R, Roy V, Rimel BJ, Mita MM. PARP Inhibition in Cancer: An Update on Clinical Development. Targeted Oncology. 2019; 14: 657–679. https://doi.org/10.1007/s11523-019-00680-2.

[34] Zhong L, Yang B, Zhang Z, Wang J, Wang X, Guo Y, *et al*. Targeting autophagy peptidase ATG4B with a novel natural product inhibitor Azalomycin F4a for advanced gastric cancer. Cell Death & Disease. 2022; 13: 161. https://doi.org/10.1038/s41419-022-04608-z.

[35] Liu Z, Huang L, Zhou T, Chang X, Yang Y, Shi Y, *et al*. A novel tubulin inhibitor, 6h, suppresses tumor-associated angiogenesis and shows potent antitumor activity against non-small cell lung cancers. The Journal of Biological Chemistry. 2022; 298: 102063. https://doi.org/10.1016/j.jbc.2022.102063.

[36] Zhou H, Shao M, Yang X, Li C, Cui G, Gao C, *et al*. Tetramethylpyrazine Analogue T-006 Exerts Neuroprotective Effects against 6-Hydroxydopamine-Induced Parkinson's Disease *In Vitro* and *In Vivo*. Oxidative Medicine and Cellular Longevity. 2019; 2019: 8169125. https://doi.org/10.1155/2019/8169125.

[37] Reheman D, Zhao J, Guan S, Xu GC, Li YJ, Sun SR. Apoptotic effect of novel pyrazolone-based derivative [Cu(PMPPSAL)(EtOH)] on HeLa cells and its mechanism. Scientific Reports. 2020; 10: 18235. https://doi.org/10.1038/s41598-020-75173-8.

[38] Liu W, Chai Y, Hu L, Wang J, Pan X, Yuan H, *et al*. Polyphyllin VI Induces Apoptosis and Autophagy via Reactive Oxygen Species Mediated JNK and P38 Activation in Glioma. OncoTargets and Therapy. 2020; 13: 2275–2288. https://doi.org/10.2147/OTT.S243953.

[39] Mao M, Zhang T, Wang Z, Wang H, Xu J, Yin F, *et al*. Glaucocalyxin A-induced oxidative stress inhibits the activation of STAT3 signaling pathway and suppresses osteosarcoma progression in vitro and in vivo. Biochimica et Biophysica Acta. Molecular Basis of Disease. 2019; 1865: 1214–1225. https://doi.org/10.1016/j.bbadis.2019.01.016.

[40] Xu Z, Zhang F, Bai C, Yao C, Zhong H, Zou C, *et al*. Sophoridine induces apoptosis and S phase arrest via ROS-dependent JNK and ERK activation in human pancreatic cancer cells. Journal of Experimental & Clinical Cancer Research: CR. 2017; 36: 124. https://doi.org/10.1186/s13046-017-0590-5.

[41] Wang N, Liu H, Liu G, Li M, He X, Yin C, *et al*. Yeast β-D-glucan exerts antitumour activity in liver cancer through impairing autophagy and lysosomal function, promoting reactive oxygen species production and apoptosis. Redox Biology. 2020; 32: 101495. https://doi.org/10.1016/j.redox.2020.101495.

[42] Bai Q, Wang Z, Piao Y, Zhou X, Piao Q, Jiang J, *et al*. Sesamin Alleviates Asthma Airway Inflammation by Regulating Mitophagy and Mitochondrial Apoptosis. Journal of Agricultural and Food Chemistry. 2022; 70: 4921–4933. https://doi.org/10.1021/acs.jafc.1c07877.